Proceedings World Geothermal Congress 2000
Kyushu - Tohoku, Japan, May 28 - June 10, 2000

SPECTRAL ANALYSIS OF AEROMAGNETIC DATA FOR GEOTHERMAL RECONNAISSANCE OF QUSEIR AREA, NORTHERN RED SEA, EGYPT

Ahmed SALEM[1], Keisuke USHIJIMA[1], Abuelhoda ELSIRAFI[2], and Hideki MIZUNAGA[1]
[1] Geophysical Exploration Lab., Faculty of Engineering, Kyushu University 6-10-1, Hakozaki, Higashi-ku, 812-8581, Fukuoka, Japan
[2] Nuclear Materials Authority of Egypt. P.O. Box 530 Maadi, Cairo, Egypt

Key Words: geothermal, magnetic, spectral analysis, modeling, Red Sea.

ABSTRACT

Dipolar aeromagnetic anomalies of the Quseir area and its extension to the offshore Red Sea have been interpreted to have a strong relation to the thermal sources of the Red Sea geothermal system. This interpretation is supported by field observations, which show that, most of these anomalies are found to be associated with diabase dyke intrusions. In order to investigate the aeromagnetic anomalies in relation to the thermal sources of the Red Sea geothermal system, spectral analysis and 2-D modeling have been applied to the aeromagnetic data. The integration of spectral analysis and 2-D modeling of aeromagnetic anomalies provided reasonable geological results, useful to further geothermal exploration. Spectral analysis suggests that the Quseir area is underlined by a Curie-point isotherm depth as shallow as 10 km. This shallow Curie-point isotherm implies a promising thermal heat flow greater than the average heat flow of the Red Sea margin. A detailed fit of the observed aeromagnetic anomalies to theoretical data by a computer model indicates that the sources could be approximated by a set of magnetic bodies of finite depth and dipping to the north east. Depths to the bottom of the magnetic bodies indicate a general increase in the geothermal gradient to 64°C/km toward to the Red Sea. This geothermal gradient indicates geothermal resources with, temperatures greater than 100°C at depths of less than 2 km. Consequently, the Quseir area is a promising area for further exploration of geothermal resources near the Red Sea in Egypt.

1. INTRODUCTION

There is considerable interest in the heat flow in the Red Sea due to the fact that the Red Sea represents an early stage in the break-up of the continental plates and their subsequent movement apart. In general, the Red Sea is clearly a region of high heat flow. More than 90 per cent of the heat flow measurements exceed the world mean and high values extend to the coasts where they are nearly twice the world mean (Girdler and Evans, 1977).

Sea floor temperatures measured in the Red Sea, show abnormally high values and sharp increases toward the central axis (Fig. 1). The geothermal gradients are higher in the southern Red Sea and concentrated in the rift zone. However, an anomalously high gradient of 12°F/100ft was also recorded in the northern Red Sea near the Quseir area, Egypt (Girdler et al., 1970).

The Quseir area and its offshore Red Sea extension (Fig. 1) have been covered by a high-sensitivity aeromagnetic survey. The end result of this survey was a map of total magnetic field intensity (Salem et al., 1999). The dipolar magnetic anomalies of this map (Fig. 2) have attracted interest from a geothermal exploration point of view. These anomalies were expected to have a strong relationship to the thermal sources of the Red Sea geothermal system. This expectation was supported by field observations, which show that the basement rocks of Quseir area are intensively intruded by diabasic dykes.

At the Curie temperature, a substance loses its magnetic polarization. Consequently, it may be possible to locate a point on the isothermal surface by determining the depth to the bottom of a polarized rock mass (Byerly and Stolt, 1977). In an attempt to study the possible relationship of aeromagnetic anomalies to the thermal sources of the Red Sea geothermal system and to help characterize the geothermal setting of the Quseir area, we estimated the depths to the Curie-point isotherm based on spectral analysis and 2-D modeling techniques.

2.TOTAL FIELD MAGNETIC ANOMALY MAP

A high-resolution aeromagnetic survey over the Quseir area and its offshore extension to the Red Sea was conducted in 1996. Figure 2 shows a map of aeromagnetic anomalies flown at 120 m terrain clearance. The flight spacing was 1 km for normal flight lines and 5 km for tie lines. The map is contoured at 10 gamma (nT) intervals and has the regional geomagnetic field (IGRF 1995), and the effects of diurnal magnetic variations removed. The map gave the first insight into the segregation of the aeromagnetic data into two regions, land area and offshore area. The two regions can be distinguished on the basis of the variation in density of the contour lines, which reflect the variations in intensity of aeromagnetic data. A concentration of high magnetic anomalies is seen on the onshore part of the surveyed area. There are NW-SE to NNW-SSE alignments of a very high intensity and short wavelength anomalies. The wavelength of the anomalies gets progressively longer towards the offshore section.

Asymmetrical dipolar magnetic anomalies aligned in the NNW and NW directions, such as the magnetic anomaly illustrated in Figure 3, have attracted interest. The positive amplitude of these anomalies extends to more than 250 nT in the onshore part of Quseir area. These anomalies were suspected to have a genetic relationship to the thermal sources of the Red Sea geothermal system. This result was reinforced by the field observations which indicated that, the basement rocks of the Quseir area are intensively intruded by diabasic dykes trending in the NNW and NW directions (Abuzeid, 1988). Consequently, the dipolar aeromagnetic anomalies are probably caused by the intrusion of these diabasic dykes. The depth extent of magnetic sources, in our case most probably dykes, can be of considerable geologic and geothermal interest. The limiting depth may be controlled, for example, by the Curie temperature isotherm (Blakely, 1995). This subject is discussed in the following section.

3. CURIE-POINT DEPTH ESTIMATION

The idea of using aeromagnetic data to estimate Curie-point isotherm depth is not new. Papers on the subject are those of Yellow Stone National Park (Battacharyya and Leu, 1975; Smith et al., 1974), parts of Airozona (Byerly and Stolt, 1977), and portions of Utah and Wyoming (Shuey et al., 1981). More

analyses have been published on Cascade Range in Central Oregon (Connard et al., 1983) and Kyushu and its surrounding areas, Japan (Okuba et al., 1985).

Estimates of the thickness of the magnetized portion of the earth's crust suggest that there are two types of lower boundaries of the layer of the magnetized rocks. The first type of boundary corresponds to vertical changes in crustal composition and the second type, where high temperatures at depth cause the rocks to lose their ferromagnetic properties i.e., below the Curie-point isotherm depth (Connard et al., 1983). The studied area, as a part from the Red Sea region, is believed to be consistent with the second type. In this work, we attempt to estimate the depth to Curie point based on spectral analysis and 2-D modeling of aeromagnetic anomalies.

3.1 Spectral Analysis

Bhattacharyya (1966) derived the expression for the power spectrum of the total magnetic field intensity anomaly over a single rectangular block as a function of the spatial frequencies u,v (radians/km) in the x and y-directions. Spector and Grant (1970) generalized that expression by assuming that the anomalies on an aeromagnetic map are due to an ensemble of vertical prisms. Thus, the energy spectrum of the map in polar coordinates is

$$< E(r,\theta) >= 4\pi^2 M^2 R_G^2 < e^{-2hr} >< (1-e^{-tr})^2 >< S^2(r,\theta) >< R_p^2(\theta) >, \qquad (1)$$

where < > indicates the expected value,

$r = (u^2+v^2)^{1/2}$ = magnitude of the frequency vector,
$\theta = \tan^{-1}u/v$ =direction of the frequency vector,
M = magnetic moment/unit depth
h = depth to the top of the prism,
t = thickness of the prism,
S = factor for the horizontal size of the prism,
R_p = factor for magnetization of the prism, and
R_G =factor for geomagnetic field direction.

Taking the average with respect to θ gives

$$< \overline{E}(r) >= 4\pi^2 M^2 \overline{R}_G^2 < e^{-2hr} >< (1-e^{-tr})^2 >< \overline{S}^2(r) >, \qquad (2)$$

where $\overline{E}, \overline{R}_{,}$ and $\overline{S}$ indicate the average over θ.

In the estimation of depths to the Curie-temperature in Oregon, for example, Connard et al. (1983) divided a magnetic survey into overlapping cells (77 x 77 km) and calculated for each cell a radially average power spectrum as in Figure 4. However, the spectrum of the map only contains depth information to a depth of length/2π (Shuey et al., 1977). If the source bodies have bases deeper than l/2π, the spectral peak occurs at frequency lower than the fundamental frequency for the map and cannot be resolved by spectral analysis. Because of the dimension of aeromagnetic data of the Quseir area (40 x 50 km), we cannot divide the magnetic data into overlapped grids and therefore, spectral analysis was applied only to the main grid. The radially averaged power spectrum of the aeromagnetic data was computed (Fig. 4). Best-fit straight lines were drawn on the spectra. Depth computations performed on the computed radial power spectrum of the aeromagnetic anomalies of the studied area (Fig. 4) revealed that the magnetic signal originates from two average depth levels of 0.76 km and 2.18km. The first depth level is the average depth of the shallow sources. Meanwhile the second depth reflects the deep-seated geologic structures.

In this work, we used the same method as Smith et al. (1974), Boler (1978) and Connard et al. (1983). They used the effect of the factor $(1-e^{-tr})$ in equation (2) to find the thickness of the deepest magnetic layer. If the map is large enough so that the low-frequency anomalies caused by the bottom of the source are included in the anomaly map (Connard et al., 1983). The factor $(1-e^{-tr})^2$ in combination with the factor e^{-2hr} introduces a peak in the spectrum, which related to the depth of the bottom of the source (Spector and Grant, 1970). When a significant spectral maximum does occur, indicating that the source bottoms are detectable, the frequency f_{max} of the spectral peak, the mean depth h to the source tops and the mean depth d to the source bottom are related by

$$f_{\max} = \frac{1}{2\pi\ (d\ -\ h)} \ln \frac{d}{h} \qquad (3)$$

The radially average power spectrum of the aeromagnetic anomalies (Fig. 4) shows a significant spectral peak. The frequency of the spectral maximum is 0.031 cycles/Km. Table 1 gives Curie-point isotherm depth estimated from the spectral maximum using the average deepest sources. The corresponding geothermal gradients and surface heat flow values are based on possible Curie-point temperatures of 580ºC using a conductivity of $2.5 Wm^{-1}{}^{o}C^{-1}$, given by Stacey (1977) as the average for igneous rocks.

3.2 Two Dimensional Modeling

As mentioned above, because of the dimension of the aeromagnetic data, spectral analysis could not be expected to provide more than one value for the depth of the Curie point isotherm. Although this value represents the average for the entire area a single value cannot assist in characterizing a geothermal setting. Accordingly, we interpreted the anomalies separately by fitting the observed data to fields calculated for dipping prisms of finite depth to the bottom using MAGMOD 3 code (Geosoft MAGMOD 3, 1990).

The main function of MAGMOD 3 is to adjust the parameters of a simple geometric model of a magnetized body, to give the "best fit" between the observed data and the calculated anomaly of the model. The quality of fit is measured objectively by calculating the weighted sum of squared deviations between the observed magnetic anomaly and the calculated anomaly at the data points. The weighted sum to be minimized is

$$S = \sum \left[W_i [T_i - (T_o + a[x_i - x_o] + b[x_i - x_o]^2) - f(x_i; x_o; M, Q, i, c, d, h, t, X, Y; L, D, S, P)]^2 \right], \qquad (4)$$

where:

x_i is the distance from the beginning of the segment of the survey line being fitted,
T_i is the observed magnetic anomaly value,
T_o is the regional background level for T at x=0,
a is the slope of the regional background,
b is the second derivative of the regional background,

f is the theoretical magnetic anomaly value,
x_o is the coordinate of the center point of the upper horizontal surface of the body,
W_i is the weight assigned to the observation at x_i .

The adjustable model parameters are magnetization (*M)*, ratio of remanence to magnetization (*Q),* remanence inclination *(i),* remanence declination *(c),* dip *(d),* depth *(h),* thickness *(t),* half width *(X), and* half length (*Y).* Meanwhile magnetic inclination *(I)*, magnetic declination *(D)*, strike perpendicular *(S)*, and line direction *(P)* are fixed parameters.

To solve the minimization problem, an iterative technique based upon the algorithm of Marquardt (1963) as described by Johnson (1969) was used. The algorithm was modified so that the Lagrange multiplier (which determines the trajectory in parameter space along which the function *S is* minimized) is adjusted automatically at each step (Geosoft MAGMOD 3, 1990). Figure 5 shows section and plane view of dipping prism (dyke) of finite depth to the bottom.

Five dipolar magnetic anomalies (labeled from A-A to E-E on Figure 6) were selected for the Curie-point depth determination (depth to the bottom). Figure 7 shows an example of the fit of the observed aeromagnetic anomaly to the theoretical data for dipping dyke of finite depth extent. The results of 2-D modeling are summarized in Table 2. The depths to the Curie-point isotherm (depth to the bottom) and the corresponding geothermal gradient and surface heat flow are listed in Table 3. The corresponding geothermal gradient and surface heat flow values are based on possible Curie-point temperatures of 580ºC using a thermal conductivity of 2.5 $Wm^{-1o}C^{-1}$, given by Stacey (1977) as the average for igneous rocks.

4. DISCUSSION

A clear interpretation of Red Sea heat flow is difficult due to the Red Seas complex tectonic and sedimentary history. It seems likely that there have been at least two stages of sea floor spreading (Girdler & Styles 1974). The first major phase of sea floor spreading was probably during the Oligocene. Large thickness of Miocene evaporites and a new phase of spreading commenced in the late Miocene/early Pliocene then covered the oceanic crust. The new oceanic crust has therefore been intruding and heating the older oceanic crust and overlying sediments for the last five million years or so (Girdler & Whitmarsh 1974).

The depth to the Curie-point isotherm computed from spectral analysis of aeromagnetic anomalies (10 km) represents the average value for the entire study area. This shallow Curie-point isotherm implies a thermal heat flow of 138 mW/m^2 greater than the average heat flow of the Red Sea margin (115 mW/m^2) given by Girdler and Evans (1977).

A detailed fit of the observed aeromagnetic anomalies to a computer model indicates that the sources may be approximated by a set of dykes striking in the NNW and NW direction and dipping to the northeast (Fig. 6). The magnetic susceptibilities range between 0.00246 and 0.00847 in emu units (Table 2). However three of the magnetic susceptibilities lie in the range of magnetic susceptibility for diabases as given by Slichter and Stern (1929).

The estimated depths to the Curie point isotherm (Table 3) suggest a melt zone below a depth of 16 km for the onshore part and getting shallower to below 8 km farther offshore. These shallow depths suggest a younger age for the intruded dykes. This suggestion agrees well with the recent work done by a South Carolina University group on dating the volcanic dykes in the Red Sea. The Pliocene age has been defined for the dykes cutting the Pre-Cambrian basement in the northern Red Sea, while the dykes seem usually to have a Paleozoic or Cretaceous age in southern Red Sea (Kanes, 1982).

Depths to the bottom of the magnetic sources indicate a general increase in the geothermal gradient as 64ºC/km toward the Red Sea (Fig. 8). Geothermal gradients measured inside the Abu Shegila shallow gradient borehole (Fig. 8) show two distinct linear gradients of 30 and 50 mK/m at respective depths of 65-160 and 175-235 m probably due to a conductivity contrast of the sediments at this site (Morgan et al., 1983). Geothermal gradients measured in Duwi and Hamrawein boreholes (Morgan et al., 1983) are lower than the gradients given by this study. However these shallow sites do not appear to be representative of the deeper thermal regime.

The estimated heat flow for four sites along Wadi Ghadir, about 150km south of the Quseir area, in order of increasing distance from the Red Sea are 179, 98, 88 and 78 mW/m^2 (Morgan et al., 1983). The above values together with the heat flow values measured in the Quseir area are close and not so far from those given by this study. This implies that, the Curie temperature of 580ºC, for pure of less than 580ºC will lead to depths shallower than depths given by our study. However, the integration of spectral analysis and 2-D modeling of aeromagnetic anomalies may provide some confidence in the estimated depths to the Curie-point isotherm in this study.

The average heat flow in thermally "normal" continental regions is around 60 mW/m^2. Values in excess of about 80 -100 mW/m^2 indicate anomalous geothermal conditions (Jessop et al., 1976). In this study, anomalous geothermal conditions have been assigned to values greater than 100 mW/m^2. Accordingly, two prospects (onshore and offshore) are highly recommended for further geothermal exploration in the north Quseir area (Fig. 9). Geothermal gradients in the onshore prospect provide a source of geothermal energy, temperatures greater than 100ºC being reached at depths of less than 2 km. Geothermal gradients in the offshore prospect provide a shallow source for hydrocarbon generation. According to (Staplin, 1977), the temperature ranges for hydrocarbon generation in the northern Red Sea are from 65 ºC to 145 ºC for oil and up to 165 ºC for gas. These temperatures ranges can be found at depths between 1 to 2.2 km for oil and at depths below 2.5 km for gas.

5. CONCLUSION

This work aimed to analyze the aeromagnetic anomalies of the Quseir area and to study the possible relationship of these anomalies to the thermal sources of the Red Sea geothermal system. Analysis of aeromagnetic data enabled the following conclusions to be drawn:

(1) The integration of spectral analysis and 2-D modeling of aeromagnetic anomalies provided reasonable geological results, which are useful to further geothermal exploration.
(2) The Quseir area is underlined by an average depth of Curie-point isotherm as shallow as 10 km. This shallow

Curie-point isotherm implies a thermal heat flow greater than the average heat flow of the Red Sea margin.

(3) A detailed fit of the observed aeromagnetic anomalies to a computer model indicates that the magnetic sources may be approximated by a set of diabasic dykes dipping to the northeast.

(4) Depths to the bottom of the magnetic sources indicate a general increase in the geothermal gradient of 64ºC/km toward the Red Sea. This provides a source of geothermal energy, temperatures greater than 100ºC being reached at depths of less than 2 km. Consequently, north Quseir is a promising area for further geothermal exploration.

ACKNOWLEDGMENTS

We are indebted to all staff of the Department of Airborne Geophysics of Nuclear Materials Authority of Egypt for their contribution to this study. Sincere thanks to all staff of the Exploration Geophysical Lab in Kyushu University for their contribution and support during this work. We would like to extend our thanks to Prof. Ehara of Kyushu University for his helpful advice on this study. Moreover, the authors are thankful to the anonymous reviewers for their constructive criticism, which helped to improve the manuscript to its present form.

REFERENCES

Abuzeid, H. T. (1988). *The youngest Precambrian volcanic succession of Wadi Hamrawein, Eastern Desert, Egypt.* Ph.D. Thesis. Earth Sc. and Res. Inst. South Carolina, Columbia, S. C. USA.

Bhattacharyya, B. K. (1966). Continuous spectrum of the total magnetic field anomaly due to a rectangular prismatic body. *Geophysics*, Vol. 31, pp.197-212.

Bhattacharyya, B. K., and Leu, L.K. (1975). Analysis of magnetic anomalies over Yellowstone National Park. Mapping the Curie-point isotherm surface for geothermal reconnaissance. *J. Geophys. Res.*, Vol.80, pp.461-465.

Blakely, R. J., 1995, *Potential theory in gravity and magnetic applications.* Cambridge Univ. Press. pp.307-308.

Boler, F.M. (1978). *Aeromagnetic measurements, magnetic source depths and Curie point isotherm in the Vale-Omyhee, Oregon.* M.S. thesis, Oregon State Univ., Corvallis.

Byerly, P.E., and Stolt, R.H. (1977). An attempt to define the Curie point isotherm in northern and central Arizona. *Geophysics*, Vol.42, pp.1394-1400.

Connard, G., Couch, R., and Gemperle, M. (1983). Analysis of Aeromagnetic measurements from the Cascade Range in central Oregon. *Geophysics*, Vol.48, pp.376-390.

Geosoft MAGMOD 3. (1990). *Geosoft 2D mapping system documents.* Geosoft Inc., Toronto, Canada.

Girdler, R.W. (1970). A review of Red Sea heat flow. *Phil. Trans. Roy. Soc. Lond.,* Vol. 267, No.1181, pp.191-203.

Girdler, R.W. and T.R. Evans. (1977). Red Sea heat flow. *Geophys. J. the Roy. Astr. Soc.*, Vol.51, pp.245-251.

Girdler, R.W. and Styles, P. (1974). Two-Stage Red Sea floor spreading, *Nature*. Vol.247, pp.7-11.

Girdler, R.W. and Whitmarch, R.B. (1974). Miocene evaporites in Red Sea cores and their relevance to the problem of the width and age of oceanic crust beneath the Red Sea. *Initial Rep. Deep Sea Drilling*, Project 23, pp.913-921, US Govt. Printing Office, Washington DC.

Jessop, A.M., Hobart, M.A., and Sclater, J. G., (1976). The world heat flow data collection 1975. *Geothermal Services of Canada*. Geotherm Ser., Vol. 50, pp. 55-77.

Johnson, W. W. (1969). A least-squares method of interpreting magnetic anomalies caused by two-dimensional structures. *Geophysics*, Vol.34, pp.65-74.

Kanes, W. H. (1982). On the geology of the Red Sea of Egypt. *Proceeding of the Egyptian petroleum Exploration Society (EPEX).* Cairo, Egypt.

Marquardt, D. W. (1963). An algorithm for least-squares estimation of non-linear parameters. *Journal of Society Industrial Applied Math,* Vol.11, pp. 431-441.

Morgan, P., Boulos, F.K. and Swanberg, G.A. (1983). Regional geothermal Exploration in Egypt. *Geophysical Prospecting,* Vol. 31, pp.361-376.

Okubo, Y., Graf, R.J., Hansent, R. O., Ogawa, K. and Tsu, H. (1985). Curie point depths of the island of Kyushu and surrounding areas Japan. *Geophysics*, Vol.53, pp.481-494.

Shuey, R.T., Schellinger, D.K., Tripp, A.C., and Alley, L.B. (1977). Curie depth determination from aeromagnetic spectra. *Geophys. J. the Roy. Astr. Soc.*, Vol.50,pp.75-101.

Slichter, L.B. and Stearn, H.H. (1929). Am. Inst. Mining Met. Engrs., Trans.

Salem, A., Elsirafi, A. and Ushijima, K. (1999). Design and application of high-resolution aeromagnetic survey over Gebel Duwi area and its offshore extension, Egypt. *Memoirs of the Graduate School of Engineering, Kyushu Univ.,*Vol. 59, No.3,pp.201-213.

Smith, R.B., Shuey, R.T., Fridline, R.O., Otis, R.M., and Alley, L. B. (1974). Yellowstone hot spot. New magnetic and seismic evidence. *Geology*, Vol. 2, pp.451-455.

Spector, A., and Grant, F.S. (1970). Statistical models for interpreting aeromagnetic data. *Geophysics*, Vol.35, pp. 293-302.

Stacey, F. D., (1997). Physics of the Earth: NewYork, John Wiley and Sons, 2nd ed., 414pp.

Stalpin, F. L., (1977). Interpretation of thermal history from color of particulate organic matter-a review: *Paleontology*, Vol.1, pp.9-18.

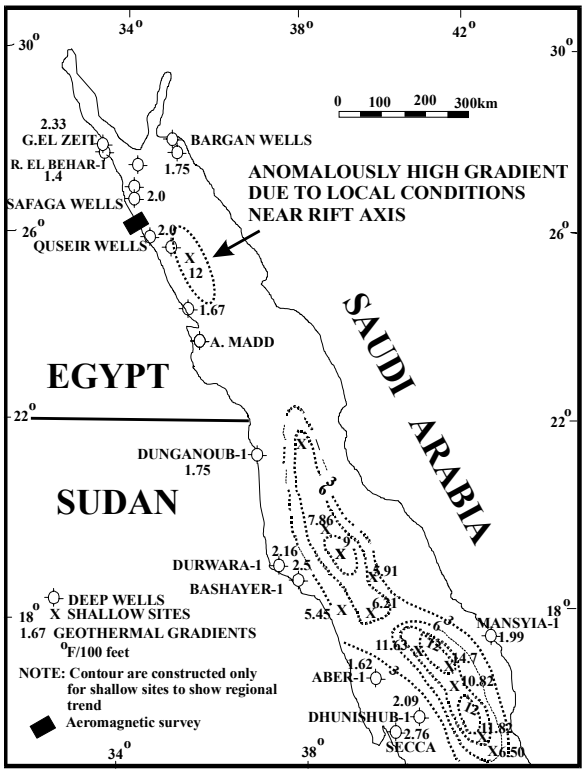

Figure 1: Geothermal Gradient Map of Red Sea (after Girdler et al.,1970)

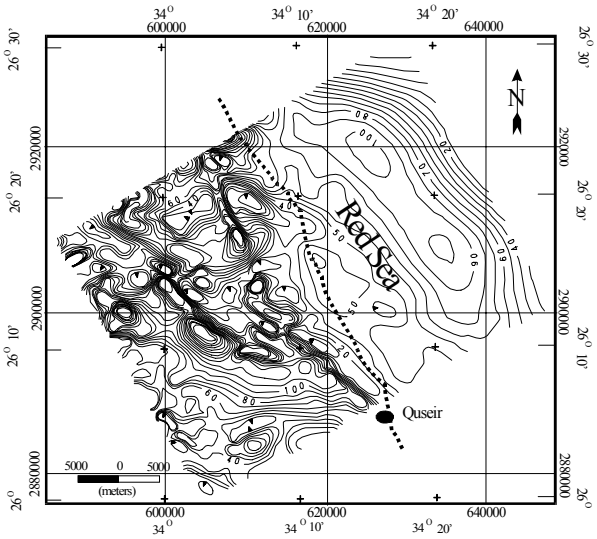

Figure 2: Aeromagnetic Contour Map of Qusier Area (Contour Interval 10 nT, after Salem et al.,1999)

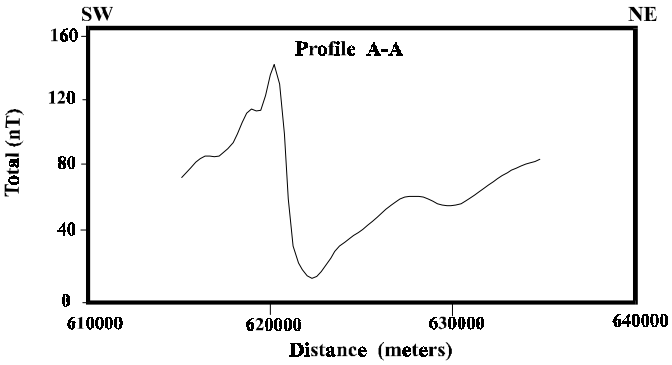

Figure 3: Example of Dipolar Aeromagnetic Anomaly

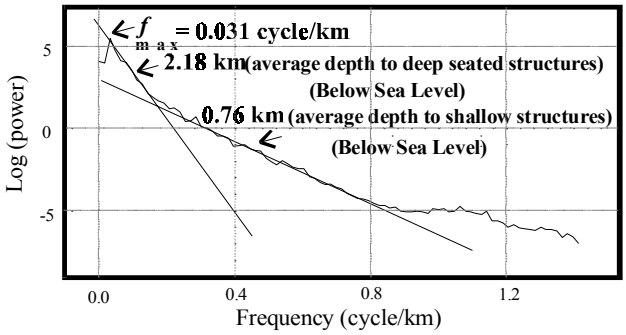

Figure 4: Power Spectrum of Aeromagnetic Anomalies

Table 1: Depth to the Curie-Point Isotherm and Corresponding Geothermal Gradient and Surface Heat Flow, Based on Spectral Analysis of Aeromagnetic Anomalies

Source Depth (Km BSL)		Curie Depth (Km BSL)	Vertical temp Gradient (°C/k)	Surface Heat Flow (mW/m^2)
Shallow	Deep			
0.76	2.18	10	55.3	138.25

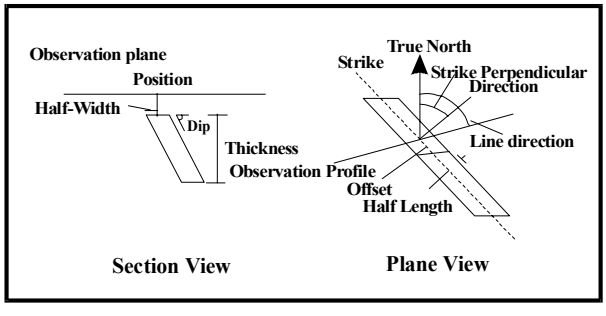

Figure 5: Section and Plane View of Dyke Body

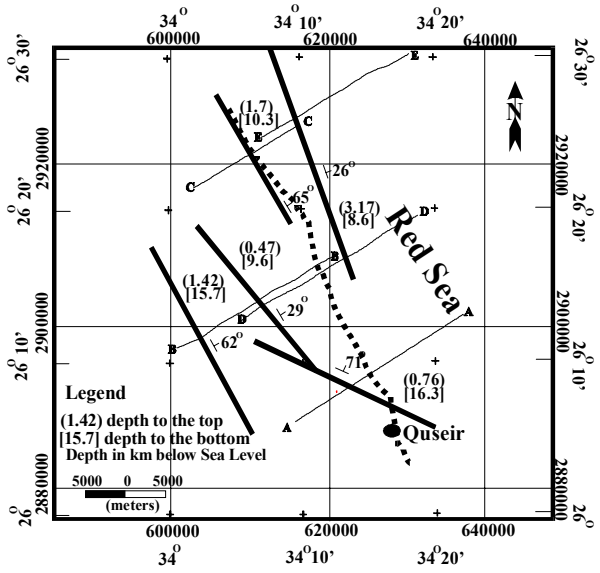

Figure 6: Interpreted Dykes Based on 2-D Modeling of Aeromagnetic Anomalies

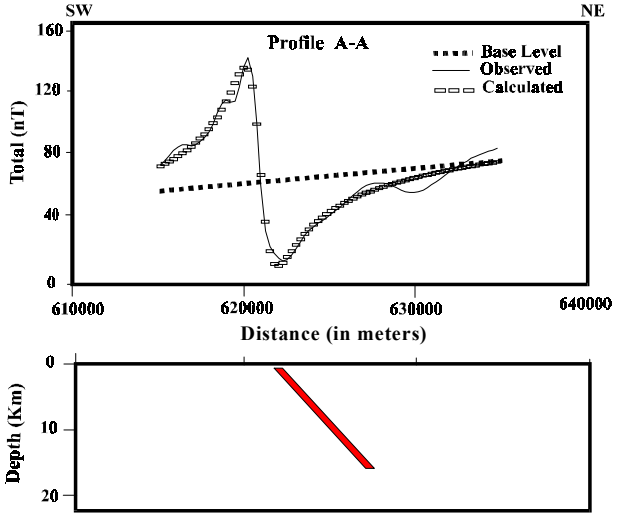

Figure 7: Example of 2-d Modeling of Aeromagnetic Data

Table 2: Results of 2-D modeling of Aeromagnetic Data

Anomaly	Strike	Depth to Top (Km BSL)	Half Width (Km)	Half Length (Km)	Dip	Susceptibility (emu)
A-A	N66°W	0.763	0.231	11.550	N71°E	0.00357
B-B	N30°W	1.427	0.397	14.359	N62°E	0.00705
C-C	N30°W	1.775	0.810	7.398	N65°E	0.00246
D-D	N42°W	0.478	0.467	11.376	N29°E	0.00847
E-E	N20°W	3.178	1.095	15.000	N26°E	0.00673

Table 3: Depth to the Curie-Point Isotherm and Corresponding Geothermal Gradients and Surface Heat Flow, Based on 2-D Modeling

Anomaly	Depth to bottom (Km BSL)	Vertical temp Gradient (°C/Km)	Surface heat flow mW/m^2
A-A	16.3	33.9	84.8
B-B	15.7	35.2	88.0
C-C	10.3	53.7	134.2
D-D	9.6	57.6	144
E-E	8.6	64.3	160.7

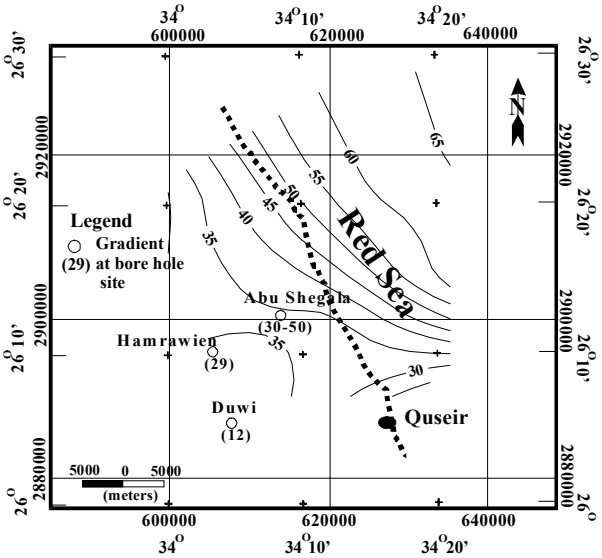

Figure 8: Geothermal Gradients Contour Map of Quseir Area (Contour Interval 5 °C/km)

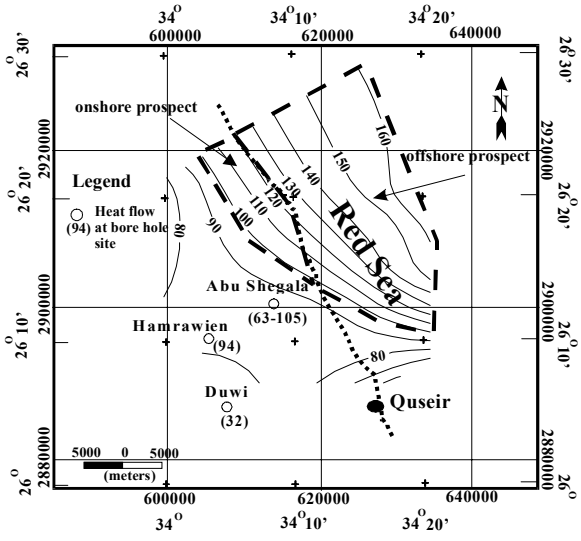

Figure 9: Surface Heat Flow Contour Map of Quseir Area (Contour Interval 10 mW/m^2)